



LAWRENCE  
LIVERMORE  
NATIONAL  
LABORATORY

# Progress on a New Integrated 3-D UCG Simulator and its Initial Application

J. J. Nitao, D. W. Camp, T. A. Buscheck, J. A.  
White, G. C. Burton, J. L. Wagoner, M. Chen

September 22, 2011

International Pittsburgh Coal Conference  
Pittsburgh, PA, United States  
September 12, 2011 through September 15, 2011

## **Disclaimer**

---

This document was prepared as an account of work sponsored by an agency of the United States government. Neither the United States government nor Lawrence Livermore National Security, LLC, nor any of their employees makes any warranty, expressed or implied, or assumes any legal liability or responsibility for the accuracy, completeness, or usefulness of any information, apparatus, product, or process disclosed, or represents that its use would not infringe privately owned rights. Reference herein to any specific commercial product, process, or service by trade name, trademark, manufacturer, or otherwise does not necessarily constitute or imply its endorsement, recommendation, or favoring by the United States government or Lawrence Livermore National Security, LLC. The views and opinions of authors expressed herein do not necessarily state or reflect those of the United States government or Lawrence Livermore National Security, LLC, and shall not be used for advertising or product endorsement purposes.

# Progress on a New Integrated 3-D UCG Simulator and its Initial Application

John J. Nitao, \*David W. Camp, Thomas A. Buscheck, Joshua A. White, Gregory C. Burton,  
Jeffrey L. Wagoner, and Mingjie Chen  
Lawrence Livermore National Laboratory

\* Contact information: L-223, P.O. Box 808, Lawrence Livermore National Laboratory,  
Livermore, CA, 94550, U.S.A., camp2@llnl.gov, phone: 925-423-9390

## Abstract

A comprehensive simulator is being developed for underground coal gasification (UCG), with the capability to support site selection, design, hazard analyses, operations, and monitoring (Nitao et al., 2010). UCG is computationally challenging because it involves tightly-coupled multi-physical/chemical processes, with vastly different timescales. This new capability will predict cavity growth, product gas composition and rate, and the interaction with the host environment, accounting for site characteristics, injection gas composition and rate, and associated water-well extraction rates. Progress on the new simulator includes completion and system integration of a wall model, a rock spalling model, a cavity boundary tracking model, a one-dimensional cavity gas reactive transport model, a rudimentary rubble heat, mass, and reaction model, and coupling with a pre-existing hydrology simulator. An existing geomechanical simulator was enhanced to model cavity collapse and overburden subsidence. A commercial computational fluid dynamics (CFD) code is being evaluated to model cavity gas flow and combustion in two and three dimensions.

Although the simulator is midway in its development, it was applied to modeling the Hoe Creek III field test (Stephens, 1981) conducted in the 1970s, in order to evaluate and demonstrate the simulator's basic capabilities, gain experience, and guide future development. Furthermore, it is consistent with our philosophy of incremental, spiral software development, which helps in identifying and resolving potential problems early in the process. The simulation accounts for two coal seams, two injection points, and air and oxygen phases. Approximate extent and shape of cavity growth showed reasonable agreement with interpreted field data. Product gas composition and carbon consumed could not be simultaneously matched for a given set of parameter values due to the rudimentary rubble model currently used, although they can be matched using separate parameter sets. This result is not surprising and confirms plans for a more sophisticated rubble model as our next step, as well as adding geomechanical collapse modeling and higher accuracy cavity gas reactive transport models. The results are very encouraging and demonstrate that our approach is sound.

## 1 Introduction

### 1.1 Overview of Underground Coal Gasification (UCG)

Coal is the most widely distributed energy source in the world, supplying 27% of worldwide demand in 2007, second only to oil. As oil reserves decline, reliance on coal is expected to continue to rise, supplying 29% of worldwide energy demand by 2030, when it will nearly overtake oil (IEA, 2009). Because the combustion of coal emits 1.3 times more CO<sub>2</sub> than oil and 1.7 times more than gas, the increasing reliance on coal poses a major challenge to the need to reduce greenhouse gas emissions. For this and other reasons, underground coal gasification (UCG) has emerged as a promising option for the future use of coal because it affords clear advantages in the deployment of carbon capture and sequestration (CCS), in addition to reducing other environmental and worker-safety impacts of coal mining and conversion.

UCG is a technology to economically access deep and/or unmineable coal seams by extracting those energy reserves through production of synthetic gas (syngas) for power generation, production of synthetic liquid fuels, natural gas, and chemicals. Coal is gasified *in-situ* from coal seams (Figure 1) to produce an energy-rich gas: H<sub>2</sub>, CO, CH<sub>4</sub>, and CO<sub>2</sub>, which can be separated and stored at lower total cost. UCG can eliminate or reduce environmental impacts associated with mining, processing, and burning of coal, such as land disturbance, acid-water discharge, solid-waste handling, emissions of dust, pollutants, and greenhouse gases, and significantly reduces the water demands for conversion and cooling.

A typical UCG module involves an injection well and a production well, which are "linked" with a conduit for the injected gasses, consisting of either air or O<sub>2</sub> and (sometimes) steam (Figure 2). After combustion is initiated, the combustion zone propagates between the injection and production well in either a forward or reverse direction, affected by tightly-coupled multi-physical/chemical processes in the coal seam and adjoining rock (Figure 3).

The combustion zone occurs in a cavity that is partially filled with spalled/caved coal and (possibly) caprock rubble from the roof of the cavity (Figure 2). Cavity growth depends on many factors, some of which can be controlled, such as the injection rates of air (or O<sub>2</sub>) and steam, as well as natural-system factors, including the thermal-hydrological-chemical-mechanical (THCM) properties of the host coal/rock environment. Coal/rock thermal conductivity affects heat conduction. Coal chemistry, oxygen availability, and temperature (controlled by convective and radiative heat-transfer) affect combustion and resulting heat-generation rates. Permeability (within fractures/cleats), together with the difference between hydrostatic and cavity pressure, controls water influx into the combustion zone, which affects (1) drying of coal, (2) flow of pyrolysis gas from the coal into the cavity, (3) flow of injected and product gas away from the cavity into the coal/rock, and (4) convective heat transfer in the coal/rock (Buscheck et al. 2009).

Permeability also affects natural convection that transports heat and aqueous-phase organic compounds from the cavity. Geomechanical properties of the fractures and coal/rock matrix affect the stability and caving of roof materials, influencing the accumulation of coal and rock rubble inside the cavity. Geomechanical effects will also influence large-scale subsidence and alter fracture properties as combustion proceeds. All of these effects will interact in a highly dynamic, non-linear manner, influencing the growth of the coal cavity within a heterogeneous coal/rock environment.

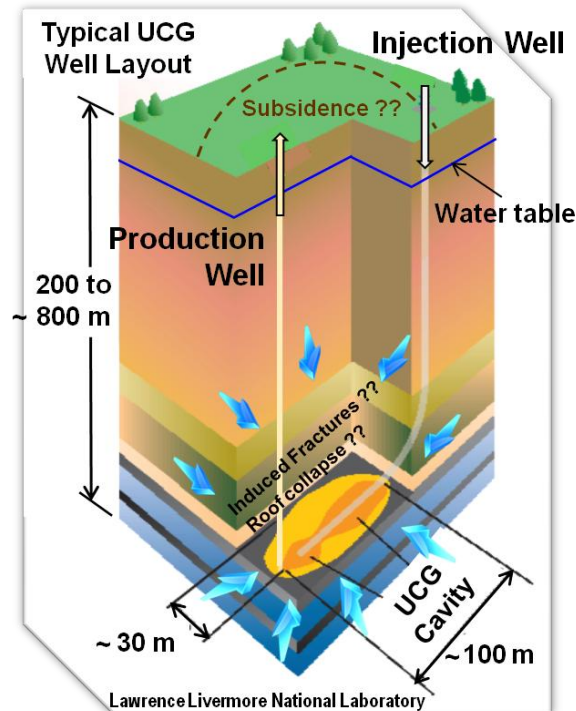


**Figure 1.** UCG gasifies *in situ* coal, using wells to feed air or pure O<sub>2</sub> and (sometimes) steam and to recover product gas. While this example depicts a Controlled Retraction Injection Point (CRIP) module (Hill 1986), many other module configurations are possible.

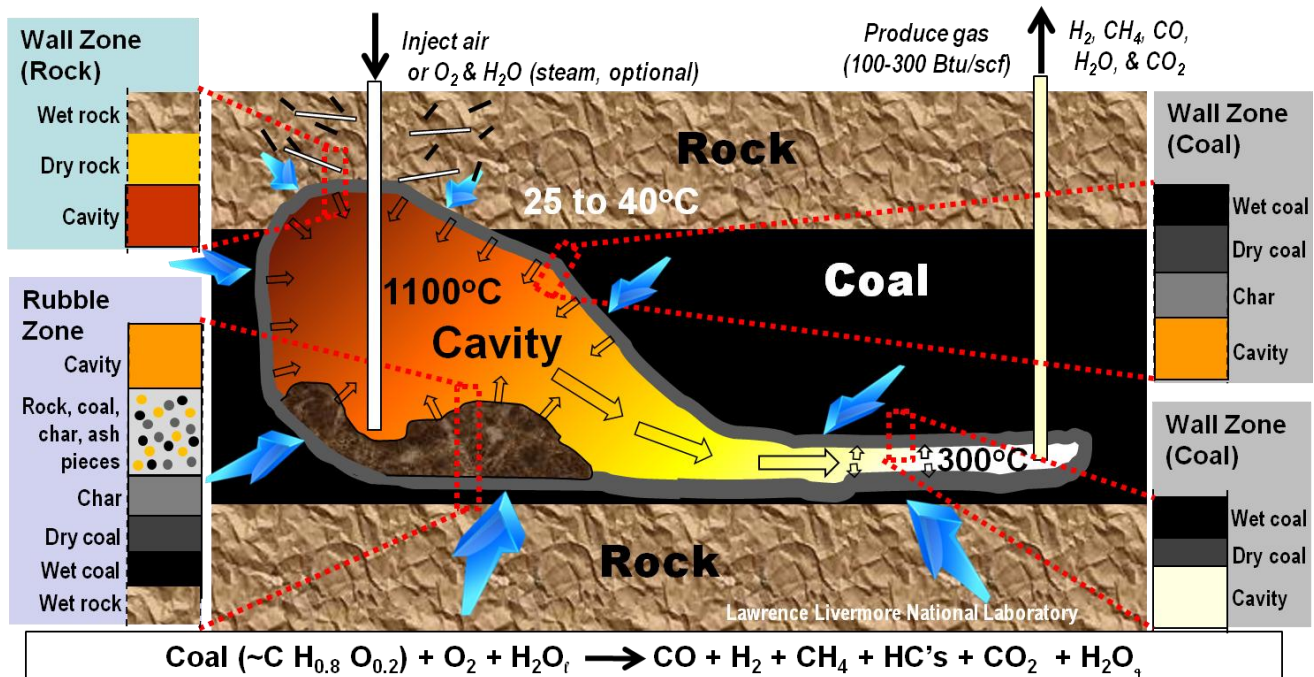


**Figure 2.** A typical cavity configuration is shown at a mid-to-late stage of a linked vertical well module. UCG involves several distinct multi-physical/chemical-process domains, including the cavity, the wall zone containing coal, the wall zone containing rock, and the rubble zone.

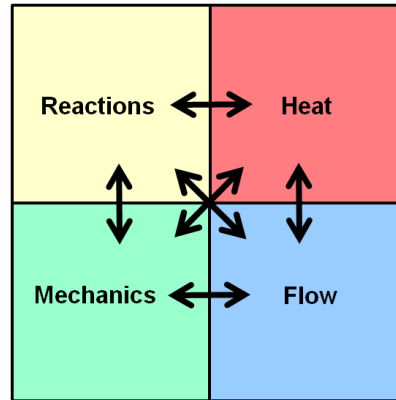


**Figure 3.** UCG involves tightly-coupled multi-physical/chemical processes, involving chemical reactions, heat and mass transfer, hydrological flow, and geomechanical behavior. These coupled processes are influenced by thermal-hydrological-chemical-mechanical (THCM) properties of the heterogeneous coal/rock environment.

## 1.2 Purpose and Requirements for a Full-Scope UCG Simulator

UCG involves very tightly-coupled multi-physical/chemical processes (Figure 3), driven by very steep temperature gradients (on the order of  $100^{\circ}\text{C}/\text{cm}$  at the cavity/coal boundary), occurring within cavities and deforming, spalling, fractured porous media, with vastly different timescales. In the vicinity of the UCG cavity (Figure 2) there are at least three major physical zones: cavity, rubble zone, and wall zone, consisting of three sub-zones: dry coal, wet coal, and rock. The boundaries between these zones move rapidly in time (a few centimeters to a few meters per day). Outside of the near-cavity region is the region where thermal-mechanical conditions are perturbed by dewatering caused by boiling and the growing cavity itself, which causes roof collapse, the creation and alteration of fractures, and (possibly) subsidence. The evolving size of the cavity formed during a UCG operation directly impacts the economic and environmental factors crucial to its success (Britten and Thorsness, 1989). The lateral dimensions of the cavity impact resource recovery by affecting the choice of spacing between modules, and the ultimate overall cavity dimensions strongly influence the hydro-mechanical response, which affects local groundwater resources and subsidence in the overburden.

UCG involves a series of engineering decisions: (1) site selection, (2) module geometry, (3) injection rates and composition (e.g., air or pure  $\text{O}_2$  and whether to inject steam), (4) location and extraction rates of sump wells, and (5) environmental monitoring. We define a full-scope UCG simulator as one that is useful for informing/guiding the full range of engineering decisions over the life-cycle of a UCG operation. A full-scope simulator must accurately predict how these decisions influence (1) cavity growth, (2) syngas composition, heating value, and rate, (3) water influx into the combustion zone and the extent to which that flux influences the local groundwater system, (4) large-scale roof collapse and subsidence, and (5) transport of UCG-generated volatile organic compounds (VOCs) away from the UCG cavity. It is also important that the monitoring program has been sufficiently designed to provide enough data to validate the predictive capability of the UCG simulator.

In addition to being an engineering-decision-making tool, a full-scope UCG simulator is required to conduct sensitivity analyses to elucidate scientific insight into the key coupled-process interdependencies that control UCG cavity growth, syngas rate, composition, and heating value, and resulting environmental responses. To conduct the requisite number of realizations for sensitivity analyses, the simulator should be computationally efficient and run on high-performance-computing (HPC) platforms. The process of gaining scientific insight will iterate with the evolving UCG simulator architecture, which we discuss in detail in the following section. Thus, another important attribute of a full-scope UCG simulator is that it has a highly flexible modular design that facilitates flexible execution. While some analyses will require full-scope integration, others will be adequately (and more efficiently) executed by exercising a specific model component, such as the geomechanical model.

In summary, a full-scope UCG simulator should be three-dimensional and include the following capabilities:

- Arbitrary cavity shape and size evolution, with local rates governed by local physical conditions
- Incorporation of the spatial geometry of the rubble zone on cavity growth
- Rubble zone reactions for entrained partially reacted coal
- Large-scale subsidence and roof collapse, computed by geomechanical codes
- Resolved cavity gas flow, using a computational fluid dynamics (CFD) code that includes turbulent gas mixing
- Detailed pyrolysis and char combustion reactions, including the influence of heterogeneous conditions (e.g., heterogeneous water influx) along the cavity wall surfaces
- Influence of local area pumping operations on water influx
- Possible transport of aqueous-phase contaminants

## 2 Simulator Architecture

### 2.1 Computational Approach

UCG involves tightly-coupled multi-physical/chemical processes, occurring in distinctly different physical domains, including the gas-filled UCG cavity, the deforming, spalling, porous wall zone (consisting of wet and dry coal and rock), and the rubble zone (consisting of partially combusted coal, ash, and rock fragments), with the coupled processes occurring over vastly different timescales. At the larger scale, coupled thermal-hydrological-geomechanical processes influence water influx and large-scale roof collapse (into the cavity) and subsidence. As shown in Figure 4, we apply a “divide and conquer” computational strategy in our UCG simulator architecture, utilizing model components (or submodels) to simulate coupled processes within the distinct physical domains and model-system components that interface the physical-domain submodels and determine the evolving boundaries between those domains. Rather than attempting to solve all of complex multi-physical/chemical processes with a single (monolithic) simulation tool, our approach is to solve them with a set of simulation tools, each designed for the respective physical domains that they represent, and then to interface their results. The model components are as follows:

- Simulator Manager (SM)
- Wall Zone Model (WZM)
- Rubble Zone Model (RZM)
- Cavity Gas and Heat Model (CGM)
- Thermal-Hydrological Model (THM)
- Geomechanical Model (GMM)
- Boundary Evolution Model (BEM)

The WZM, RZM, CGM, THM, and GMM are physical-domain model components that calculate multi-physical/chemical processes within the respective domains they represent. The SM and BEM are model-system components (rather than models of physical domains) that work to tie the physical-domain models together and track the boundaries between them. Each component of the simulator will now be described.

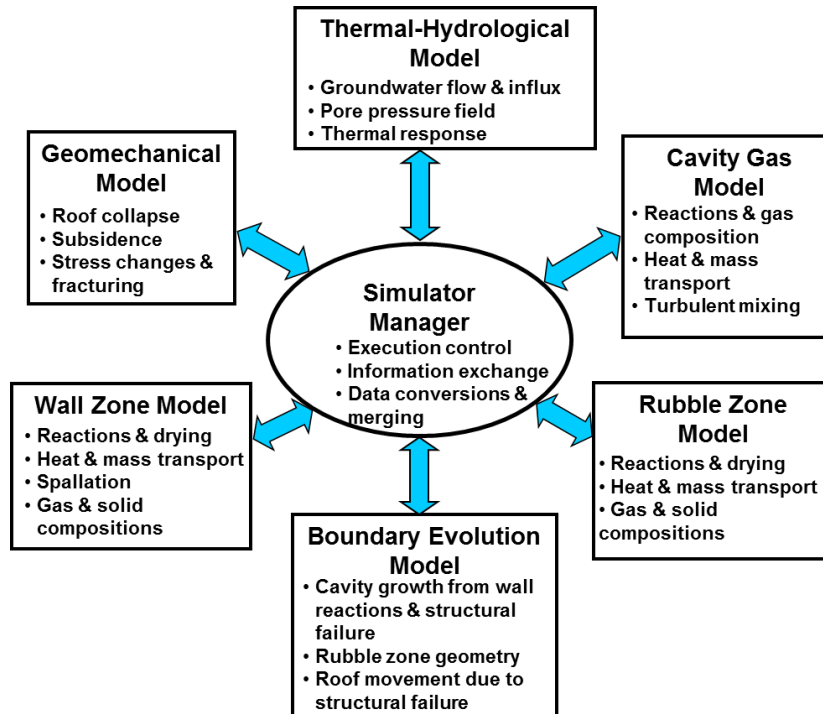


**Figure 4.** The system architecture is shown for the full-scope UCG simulator.

### 2.2 Simulator Manager (SM)

The functions of the SM are

- Control all of the physical-domain models (WZM, RZM, CGM, THM and GMM) and model-system component (BEM)
- Communicate data and information needed for interfacing respective physical-domain models
- Convert between different data formats used by the respective models

An important system-architecture goal is to the ability to “plug-in” different physical-domain models. As part of its control function, the SM must determine the time scale over which each model is called in order to meet accuracy and numerical stability requirements, yet maintain computational efficiency. In many cases, a model may pass to the SM when it should be called again, or when it may give changes or rates of change in important physical variables. For example, the GMM may indicate to the SM when it must be called again because the roof is approaching the critical stress conditions.

### 2.3 Wall Zone Model (WZM)

The WZM is responsible for all of the small-scale physical and chemical processes in the coal and rock that directly influence the combustion zone and cavity growth, including spallation. The steep temperature gradients in the wall zone result in the small-scale processes occurring within the first ten's of centimeters into the cavity wall. Most importantly, the WZM models the pyrolysis of volatile solids and combustion of carbon that results in the release and/or consumption of gas species and heat. Because of the steep gradients in temperature and composition existing there, it would be inefficient to have a finely resolved computational grid near the cavity wall. Our approach is to take advantage of the fact that fluxes are approximately normal to the cavity wall, which allows us to use an array of 1-D WZM submodels, oriented orthogonal to, and distributed along the cavity wall surface (Figure 5).

The 1-D WZM submodels are used to (1) compute mass and energy fluxes that are exchanged with the cavity gas, (2) compute mass and energy fluxes where the wall is in contact with the rubble zone, (3) exchange heat fluxes with the THM, and (4) pass the small-scale spallation rate to the BEM and RZM for computing changes in the cavity and rubble zone boundaries.

The WZM is coupled to the THM as shown in Figure 5. The ends of the 1-D wall models that point away from the wall are coupled to the THM, which is a 3-D porous-media model for groundwater flow and heat transport in the surrounding coal and rock.

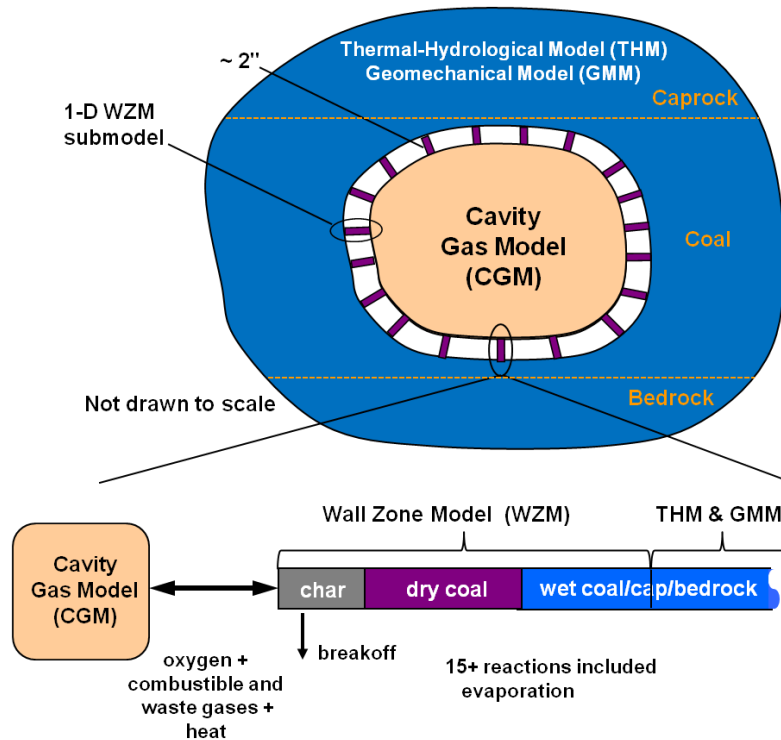


**Figure 5.** The relationships between the Wall Zone Model (WZM, Cavity Gas Model (GCM), Thermal-Hydrological Model (THM), and Geomechanical Model (GMM) are shown.

### 2.4 Rubble Zone Model (RZM)

The RZM simulates all processes within the rubble pile, consisting of rock, ash, and partially combusted coal fallen from the cavity walls. The reactions within the rubble are essentially the same as those in the 1-D WZM submodels. However, fluid flow and mass and heat transfer are more complicated because the pile is a mixture of micropores, consisting of low-permeability fragments of coal, ash, and rock, surrounded by macropores, which, because it is the space between the fragments, have a high permeability.

### 2.5 Cavity Gas Model (CGM)

The CGM encompasses all gas-phase processes within the cavity: fluid flow, mass and heat transfer, thermal radiation, and reactions. This model solves the Navier-Stokes equations, coupled with species and energy balances. Cavity combustion is highly dependent on turbulent mechanisms by which the injected gas stream mixes with the fluxes emanating from the wall due to combustion and pyrolysis, as modeled by the WZM.



## 2.6 Geomechanical Model (GMM)

The purpose of the GMM is to predict roof collapse, large-scale spallation, and large-scale subsidence due to changes in the geomechanical stress field. These events are induced by the stresses in response to changes in the cavity wall geometry and the temperature field.

## 2.7 Thermal-Hydrological Model (THM)

The THM is responsible for 3-D thermal-hydrologic flow throughout subsurface surrounding the WZM/near-cavity region, all the way out to the far-field boundaries, such as the ground surface. Away from the cavity, due to hydrogeologic heterogeneity, water flux vectors are no longer normal to the cavity wall surface. Moreover, large-scale geomechanical effects can alter formation permeability. Therefore, a fully three-dimensional computation is required, which needs to be interfaced with the GMM to determine whether significant alteration in permeability has occurred. An existing code NUFT, developed at LLNL (Nitao, 1998), is used, and coupled with the SM.

## 2.8 Boundary Evolution Model (BEM)

The BEM advances (in three dimensions) the surfaces that bound the three major physical-domain models: the cavity volume, the wall (coal/rock) zone, and the rubble zone. Note that the term “cavity volume” used here refers to the open gas-filled portion that is not occupied by rubble.

Cavity and rubble boundary movement is the result of the following effects.

- Small-scale spallation at cavity wall occurs, due to coal pyrolysis and combustion, whose rate is predicted by a 1-D WZM.
- Large-scale spallation and roof collapse can occur, whose rates are predicted by the GMM.
- Addition of ash and partially combusted coal occurs, as it falls from cavity wall.
- Rubble surface recession, volume shrinkage, and weight compaction occur due to combustion within the rubble, with the consumption rate predicted by the RZM.
- Ash will slide on rubble surface when the critical angle of repose is exceeded.
- Coal is consumed as a result of pyrolysis and combustion, although at a lower rate than in the wall zone along the cavity wall, due to reduced rates of heat and mass transfer within the rubble zone.
- Rubble can be compacted under its own weight.

## 3 Progress to Date

### 3.1 Wall Zone Model

The 1-D coal gasification model component of the WZM has been completed. It is an extension of the mathematical model of Perkins and Sahajwalla (2005, 2008). Implementation details were given by Nitao et al. (2010). A new overburden thermal rock spalling model component has been built using the approach described by Camp et al. (1980). It computes local spalling rate of rock as a function of cavity temperature, cavity pressure, *in-situ* water content, and time. Its use in the simulator is in the same manner as the 1-D coal gasification model – a series of 1-D models normal to the cavity wall, in this case, the portion that forms the overburden roof. In addition to the cavity-coal interface, 1-D coal gasification models are placed at the rubble-coal interface. Currently, a transfer coefficient approach is used for the fluid-thermal coupling with the cavity gas. In the future, coupling will be directly to a multidimensional rubble zone model.

### 3.2 Rubble Zone Model

A highly-simplified rubble zone model has been implemented, primarily for prototyping the overall simulator integration. This model gasifies an assigned percentage of spalled char instantaneously as it falls from the exposed coal face. The amount of char leftover is never gasified. The specific heat from spalled ash and rock material is stored in a rubble compartment, with each cell of the 1-D gas cavity model (which will be described below) having a rubble compartment. This heat can be used to evaporate any liquid water seeping into the cavity which is transferred to the CGM. A more sophisticated model discretized in three dimensions will be developed in the next stage of the project.

### 3.3 Cavity Gas Model

#### 3.3.1 Multidimensional CFD Cavity Gas Model (CGM)

The application of the commercial CFD code STAR-CCM is being evaluated through modeling of idealized large gas cavity geometries in two and three dimensions. Figure 6 shows results from a three dimensional model that uses approximately 4 million computational cells.



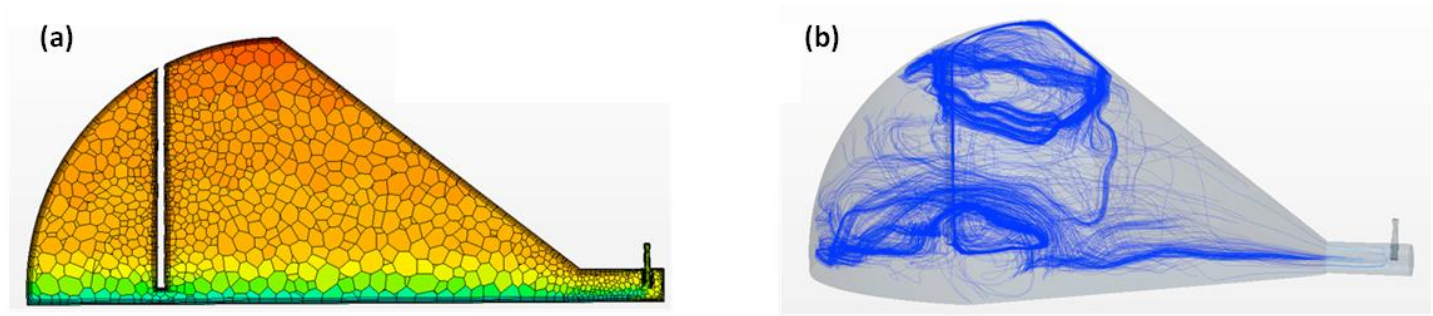


**Figure 6.** Three-dimensional model of gas flow in a large 75- x 60- x 40-m cavity is shown, including (a) temperature and (b) streamline trace through the center plane as a result of the injection air from a vertical well.

### 3.3.2 One Dimensional Cavity Gas Model (CGM)

A 1-D cavity gas model was also developed. The model can be viewed a linear series of connected compartments (see Fig. 7) in which gas reactions are calculated as a well-stirred tank. Species mass and energy are transported by advection, dispersion, and diffusion between compartments. The gas flow rate is assumed to be steady-state or quasi-steady-state. Injection rate, composition, and temperature history are specified by the user. The model then computes the gas temperature and composition at each compartment by solving the mass and energy balance equations. Each compartment is connected to seepage and rubble compartments. Multiple wall models (for coal or rock) are also coupled to each gas cavity compartment. Experimentally derived expressions for axial dispersion coefficients (Levenspiel, 1999), and steady-state mass and energy transfer coefficients are used for radial transport. Thermal radiation between the gas and walls is included. The compartment volumes and flow areas are computed from the interface positions computed by the boundary evolution model (BEM).

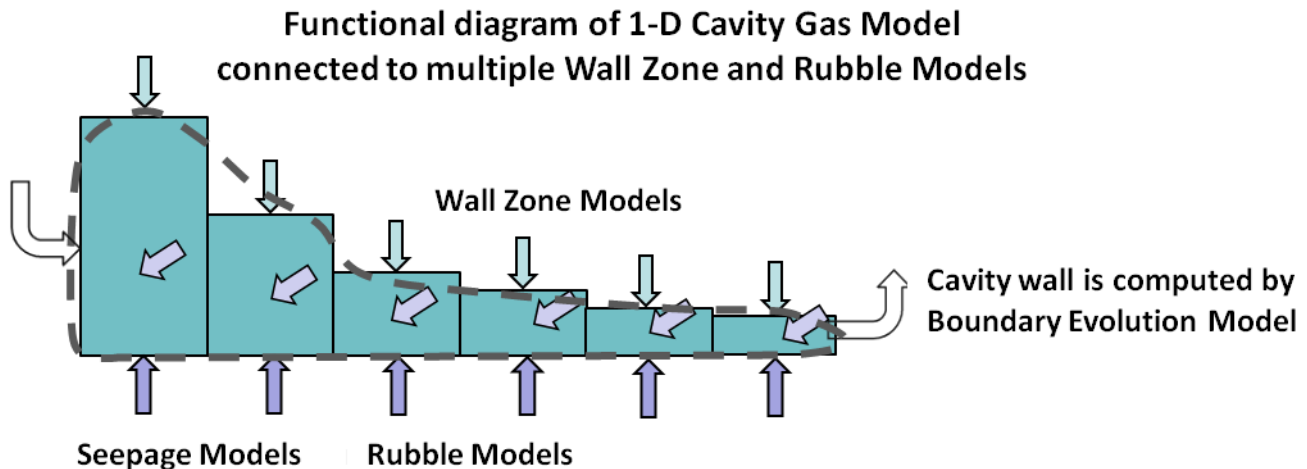


**Figure 7.** The 1-D cavity gas model consists of connected compartments whose size is determined by the BEM. Each compartment is connected to a rudimentary rubble model compartment, a seepage model, and one or more 1-D wall models.

### 3.4 Geomechanical Model (GMM)

The geomechanical module uses Geocentric, a massively parallel finite element code for geomechanical simulations (White and Borja, 2008, White, 2009; White and Borja, 2010). The model solves a governing linear momentum balance for the stress and deformation within the coal seam and surrounding host rock. It employs a continuum formulation, so that discrete features such as joints and fractures are not explicitly modeled. Rather, it is assumed that an equivalent macroscopic material model can capture the effect of persistent, small-scale features. The code shows excellent parallel scalability, and can tackle large, three-dimensional problems with tens-of-thousands to hundreds-of-millions of degrees of freedom.

In the current generation simulator, the material response is modeled using a non-associative hyperbolic Drucker-Prager elastoplasticity model. The parameters of the model are a bulk modulus, Poisson ratio, cohesion intercept, friction angle, dilatancy angle, and a parameter controlling the curvature of the yield surface. This parameter can be chosen to either reproduce a linear Mohr-Coulomb or nonlinear Hoek-Brown-type yield surface in the mean-stress/deviatoric-stress plane. The yield surface is circular on planes perpendicular to the hydrostatic axis, and no variation with Lode's angle is modeled. Later generations of the simulator will include a full three-invariant model, with more sophisticated hardening/softening behavior. For highly jointed rock with preferential orientations, we also intend to include anisotropic models.

Figure 8 illustrates a typical Geocentric simulation of the Hoe Creek III cavity geometry. The contours of plastic strain norm indicate that a collapse zone is forming in the unsupported cavity roof. At the end of the geomechanical analysis, this collapsed material becomes newly created rubble, and the cavity grows vertically from the Felix 2 up towards the Felix 1 seam.

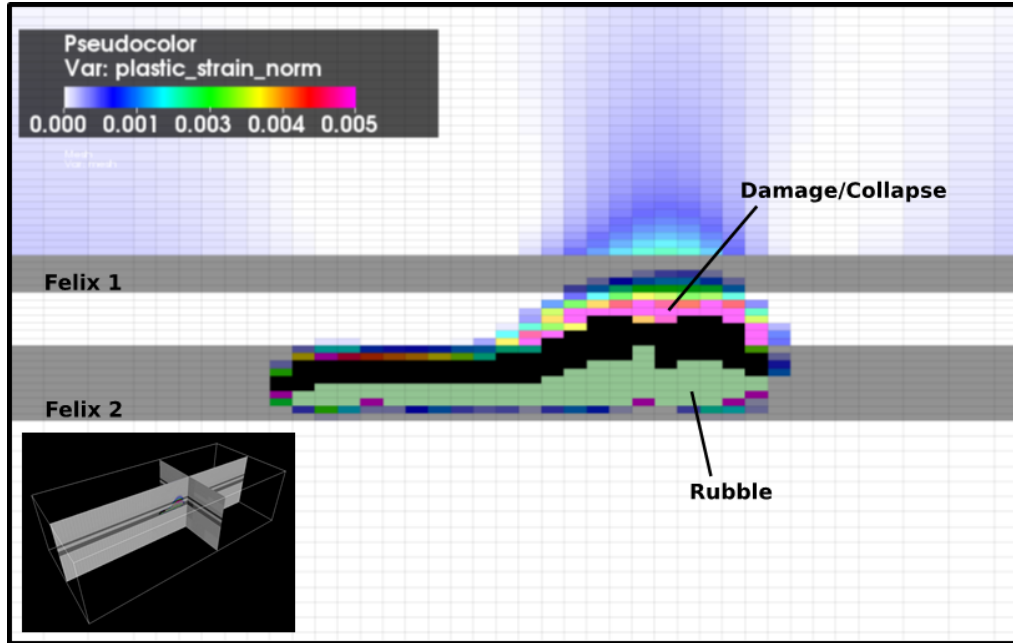


Figure 8. Typical geomechanical simulation of the Hoe Creek III cavity at one time-snapshot.

### 3.5 Thermal-Hydrological Model (THM)

The thermal-hydrological model, which is based on the NUFT code (Nitao, 1998), has been integrated into the simulator and is called roughly every few simulation hours to update the hydraulic seepage fluxes in response to the changes in the cavity geometry. Future work will involve coupling with the GMM to account for mechanically-induced permeability changes.

### 3.6 Boundary Evolution Model (BEM)

The basic capabilities of the BEM, which governs movement of cavity and rubble zone boundaries, is nearly completed, including the ability to accept fall of rock due to roof collapse, as computed by the GMM. Future work will involve tracking composition (char, rock, ash, void space) of the rubble material, for use by the RZM.

## 4 Simulation of the Hoe Creek III Field Test

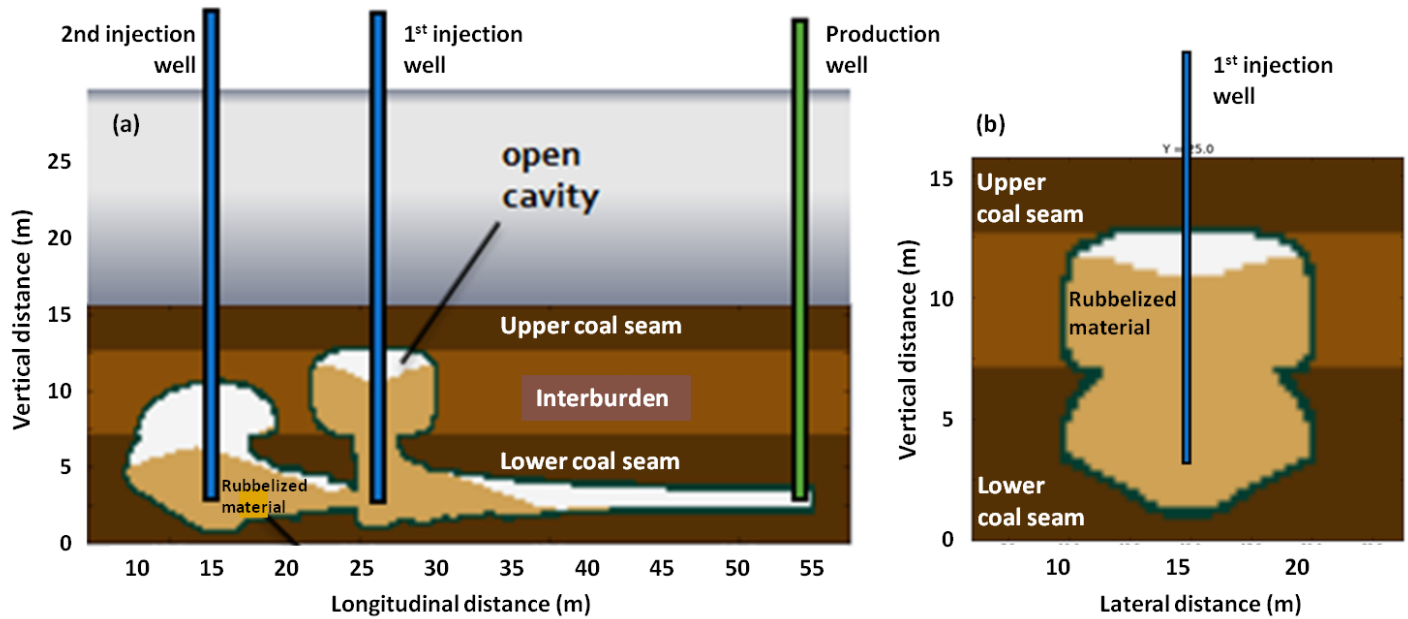
Between 1976 and 1979, Lawrence Livermore National Laboratory conducted three UCG pilot tests at the Hoe Creek Test Site, Wyoming (Stephens, 1981). A wide variety of data was carefully collected and archived:

- Detailed site design and geological characterization,
- Time-histories of injection and product gas pressure and composition,
- Thermocouple data,
- Cross-well electro-magnetic tomography (EMT),
- Extensimeters and collapse observations.

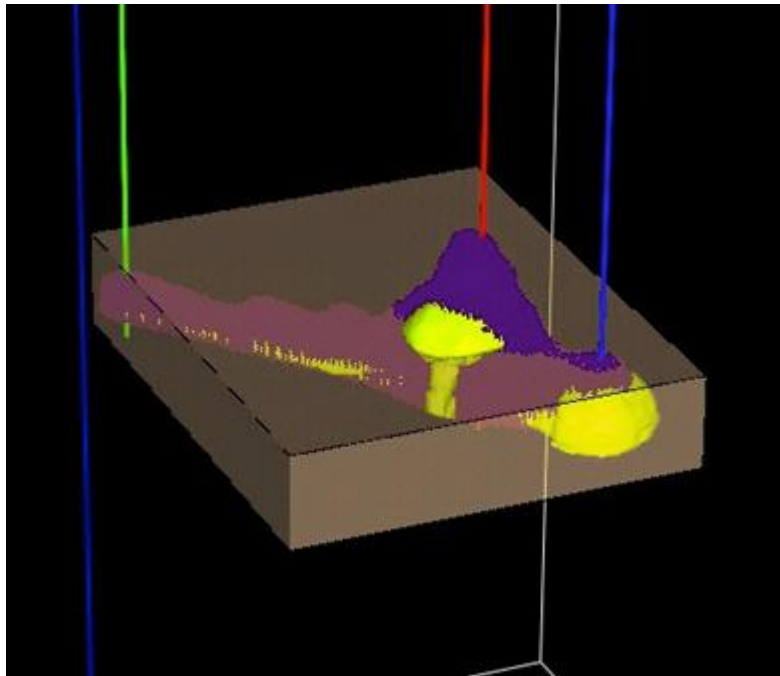
We have applied the simulator to one of these tests, at the Hoe Creek III site. Although the simulator is midway in its development, we felt that the exercise would be useful for evaluating and demonstrating the simulator's basic capabilities, gaining valuable experience, and guiding future development. Furthermore, it is consistent with our philosophy of incremental, spiral software development, which helps in identifying and resolving potential problems early in the process.

The target Felix II coal seam (the lower seam in Fig. 9) is about 7.5 m thick and has a bottom depth of 56m below the ground surface. An interburden, consisting primarily of claystone, separates Felix I from another coal seam, Felix I (the upper seam in Fig. 9) above it. After approximately one day of reverse burn linking, air was injected into the center well in the figure into Felix II from day 1 to 8. Due to plugging in this well, injection was switched to the second well from day 9 to day 15 with 45% oxygen and 50% steam injection stream. So far, we have modeled only this time period (1-15days). The actual field test lasted for a total of 55 days.

Fig. 9 shows the cavity and rubble cross-sections at 15 days showing that the cavity has reached the upper coal seam through thermal spalling of the interburden rock. In the actual test, this occurred earlier at about 10 days; spalling was perhaps possibly accelerated by geomechanical roof collapse, which is not yet treated in our model. Fig. 10 shows the three-dimensional comparison. The yellow is the cavity boundary predicted by the simulator and the brown/purple is the cavity boundary from field data interpretation.



**Figure 9.** The cavity and rubble zones simulated at day 15 of the Hoe Creek III test are shown for (a) side view and (b) cross-sectional view. The first injection phase (day 1 through day 8) consists of air injection in the first injection well. The second injection phase (day 9 through day 15) consists of a 50/50 mixture of oxygen and steam. The bottom of the lower coal seam is 56 m below the ground surface.



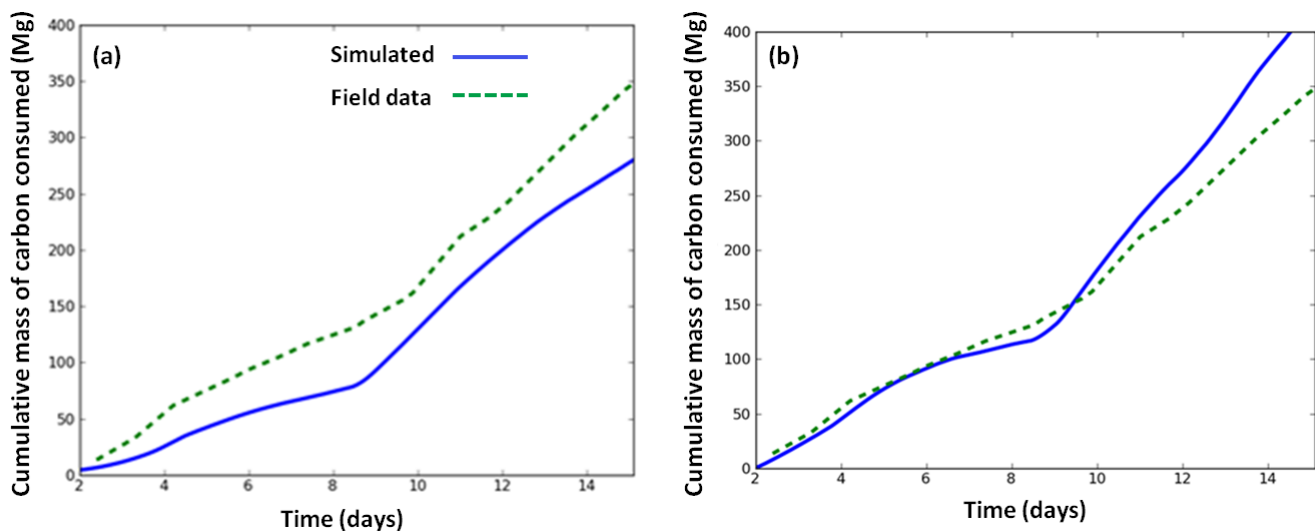
**Figure 10.** Three-dimensional view of the cavity is shown at 14 days. The yellow is the simulated cavity surface and the brown/purple is from interpreted field data.

Fig. 11 is a plot of the cumulative carbon consumed versus time based purely on the production composition for two separate cases of a parameter which governs the rate of char spallation from the combusting coal face. Char spallation is important because it strongly affects combustion rates and cavity growth direction. Our wall models spall char at the coal face when the local fraction of

initial char consumed reaches a critical user-specified value  $X_c$ . Fig. 11a is for the  $X_c=0.8$  case and Fig. 11b is for  $X_c=0.4$ . By looking at the slopes of the curves, the carbon consumption rate is seen to be too low for the  $X_c=0.8$  case during the early phase (day 2-8) and about right in the later phase (8-15). The case  $X_c=0.4$  is about right in the early phase and too high in the later phase.

This discrepancy can be explained. The value  $X_c=0.4$ , we feel, is the correct one. The overprediction in the later phase is due to the rudimentary rubble zone model, which instantaneously combusts spalled char under cavity gas conditions. Char oxidation will dominate in the presence of oxygen over the other gasification reactions, producing  $\text{CO}_2$ . However, in real-life a significant amount of char will be buried under falling rock, away from the main oxygen stream, and will react primarily by non-oxidative gasification, producing more  $\text{H}_2$  and  $\text{CO}$ . Therefore, the predicted product gas composition for the  $X_c=0.4$  case is poor, predicting  $\text{H}_2$  and  $\text{CO}$  production that are much too low and  $\text{CO}_2$  that is too high.

Fig. 12 shows that the product composition for the  $X_c=0.8$  case, which gives the correct trends. This is because most of the char reacts in this case within the coal by non-oxidative gasification, except at the exposed char face. This situation is similar to the char buried within the rubble. Fig. 12 also shows the comparison with the molar production rate of gas for the same  $X_c=0.8$  case. The discrepancy with field data is not as much in the  $X_c=0.4$  case because more carbon is produced. However, the discrepancy in production rate is still there and consists primarily of more water vapor produced in the field test than our prediction. We tried increasing the seepage flux, but this led to much lower cavity growth rates than seen in the field test. It is possible that the unaccounted water vapor arises from higher evaporation of seepage resulting from thermal energy stored from the earlier reverse combustion ignition stage, which we have not expended any great effort to model accurately. The oscillations in the graph are due to rapid changes in mass and energy caused by rock spallation.



**Figure 11.** The time history of cumulative mass of consumed carbon is plotted. The simulated results are compared with those determined from field data for (a) the case for  $X_c=0.8$  and (b) the case for  $X_c=0.4$ .

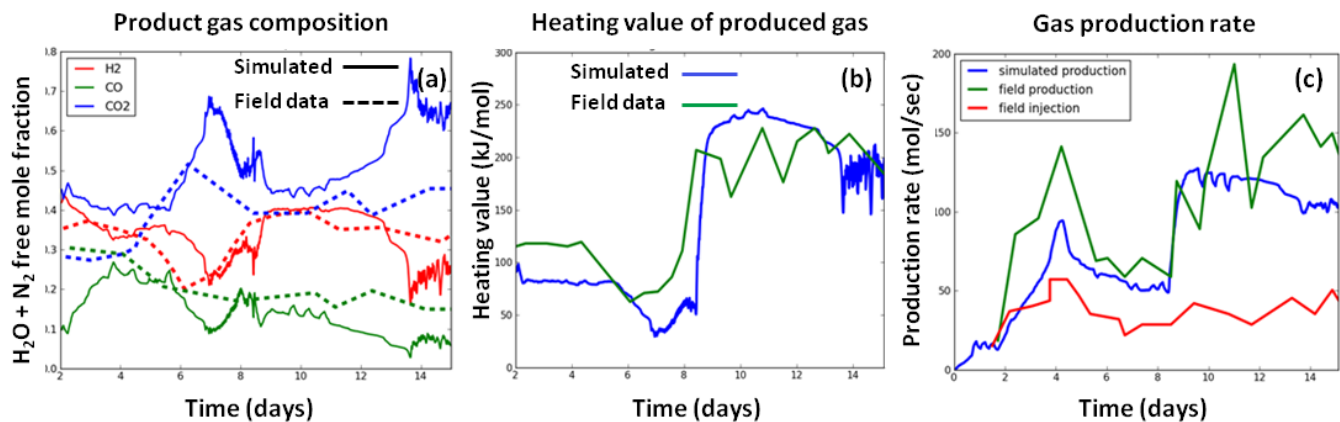


**Figure 12.** The time history of (a) product gas composition, (b) heating value of produced gas, and (c) gas production rate are plotted. The simulated results for the  $X_c=0.8$  case are compared with those determined from field data.

## 5 Future Work

Future efforts will focus on developing an enhanced rubble zone model, integrating the geomechanical and the CFD cavity gas models. It is anticipated that completion and testing of all model components will be completed within the next twelve months. Comparisons with field tests will continue. Sensitivity analyses will be conducted to identify and quantify the key coupled-process interdependencies that control UCG cavity growth, syngas rate, composition, and heating value, and resulting thermal-hydrological and geomechanical responses required to assess environmental risks. This will involve use of the full-scope UCG simulator, as well as the individual physical-domain models.

## 6 Summary and Conclusions

Despite the simplifications made, the results are highly encouraging and demonstrate that our approach is sound. We have demonstrated that the simulator can model a challenging problem with changing well injection schedules and combustion across multiple coal seams. The discrepancies with field can be understood in light of the simplified treatment of spalled char reactions and lack of a roof collapse model. More accurate modeling requires an improved rubble zone model, geomechanical coupling, and 3-D fluid flow and combustion modeling. The results so far show that our divide-and-conquer approach is feasible despite the challenge of disparate time and length scales, and the complexities, inherent in the UCG process.

## Acknowledgements

This work was performed under the auspices of the U.S. Department of Energy by Lawrence Livermore National Laboratory under contract DE-AC52-07NA27344.

## 7 References

- Britten, J.A. and Thorsness, C.B. "A model for cavity growth and resource recovery during underground coal gasification", *In Situ*, 13 (1 & 2), 1-53, 1989.
- Buscheck, T.A, Hao, Y, Morris, J.P, and Burton, E.A. "Thermal-hydrological sensitivity analysis of underground coal gasification", Proceedings of the 2009 International Pittsburgh Coal Conference, Pittsburgh PA, September 20-23, 2009.
- Camp, D.W, Krantz, W.B, and Gunn, R.D. A water-influx model for UCG with spalling-enhanced drying, Proc. 15<sup>th</sup> Intersociety Energy Conversion Engineering Conference, Seattle, WA August 18-22, 1980.
- Levenspiel, O. *Chemical Reaction Engineering*, 3<sup>rd</sup> ed., John Wiley & Sons, 1999.
- Nitao, J.J. Reference manual for the NUFT flow and transport code, version 3.0, Lawrence Livermore National Laboratory, UCRL-MA-130651-REV-1, 1998.
- Nitao, J.J., Buscheck, T.A., Ezzedine, S.M., Friedman, S.J., Camp, D.W. An Integrated 3-D UCG Model for Predicting Cavity Growth, Product Gas and Interactions with the Host Environment, Proc. Pittsburg Coal Conf. 2010, Istanbul, Turkey, Oct. 11-14, 2010.
- Perkins, G. and Sahajwalla, V. A mathematical model for the chemical reaction of a semi-infinite block of coal in underground coal gasification, *Energy Fuels*, 19, 1679–1692, 2005.
- Perkins, G. and Sahajwalla, V. Steady-state Model for estimating gas production from underground coal gasification, *Energy & Fuels*, 22, 3902-3914, 2008.
- Stephens, D.R. "The Hoe Creek experiments: LLNL's underground coal gasification project in Wyoming", Lawrence Livermore National Laboratory, Livermore, CA, UCRL-53211, 1981.
- Thorsness, C.B. and Britten, J.A. A mechanistic model for axisymmetric UCG cavity growth, Lawrence Livermore National Laboratory, UCRL-94419 (NTIS no. DE87011570), 1986.
- White, J.A. and Borja, R.I. "Stabilized low-order finite elements for coupled solid-deformation/fluid-diffusion and their application to fault zone transients", *Computer Methods in Applied Mechanics and Engineering*, 197(49-50):4353–4366, 2008.
- White, J.A. "Stabilized finite element methods for coupled flow and geomechanics", PhD thesis, Stanford University, Stanford, CA, 2009.
- White, J.A. and Borja, R.I. "Block-preconditioned Newton-Krylov solvers for fully-coupled flow and Geomechanics", *Computational Geosciences*, in review, 2010.